

## Two-step template-free route for synthesis of TiO<sub>2</sub> hollow spheres

Zhenfeng Zhu · Zuoli He · Junqi Li ·  
Jiaqi Zhou · Na Wei · Dianguang Liu

Received: 29 April 2010/Accepted: 14 August 2010/Published online: 31 August 2010  
© Springer Science+Business Media, LLC 2010

**Abstract** The TiO<sub>2</sub> hollow microspheres were prepared by microwave-assisted solvothermal treatment without template. The morphology and the phase of TiO<sub>2</sub> hollow microspheres were characterized by X-ray diffraction (XRD), field emission scanning electron microscopy (FE-SEM), high resolution transmission electron microscopy (HR-TEM), and BET surface areas. The results show that the particles have hollow structures and the shell was covered by nanocrystals and have higher specific surface area. The possible formation mechanism of hollow TiO<sub>2</sub> spherical structures has simply been proposed. The activity was evaluated by the photocatalytic degradation of methyl orange (MO). The results show that the particles having specific surface area show higher photocatalytic activity. It can be attribute to the doped F atoms and the creation of oxygen vacancies.

### Introduction

Three-dimensional (3D) structure of hollow spherical nanoparticles has many excellent and interesting performances that attract significant attention nowadays [1–4]. Among them, hollow spheres have increasingly attracted tremendous interest as a special class of materials compared to the solid counterparts, due to their higher specific surface area, lower density, better permeation, and greater light-harvesting capacity [5, 6]. And the structure of TiO<sub>2</sub> hollow spheres has been used in many areas, including

photocatalysts, electrochromic devices, gas sensor, dye-sensitized solar cells, biomedical implants, and field emitters [7–10]. It has been reported about the preparation of hollow TiO<sub>2</sub> microspheres by a spray pyrolysis technique [11] or by a sol-gel reaction with introducing templates [12]. Recently, the preparation of hollow TiO<sub>2</sub> microspheres by hydrothermal method without introducing templates was also published [13]. Zeng group [14] also reported an approach to prepare hollow anatase TiO<sub>2</sub> nanospheres using titanium tetrafluoride as the starting materials via Ostwald ripening process. Li et al. [15] have prepared hollow TiO<sub>2</sub> spheres using potassium titanium oxalate as the precursor, and the photocatalytic performance of hierarchical structures was significantly improved due to their 3D structure. Self-organized polycrystalline F-doped TiO<sub>2</sub> hollow spheres were also synthesized via hydrothermal process at 180 °C for 20 h and the photocatalytic activity was clearly enhanced [16]. Nevertheless, there are few reports on the formation of TiO<sub>2</sub> hollow spheres using TiO<sub>2</sub> microspheres as the starting materials via microwave-assisted solvothermal process. It is well-known that surface oriented erosion of titanium directed by the electric field plays great roles in the formation of TiO<sub>2</sub> nanotubes. We deduce that TiO<sub>2</sub> hollow spheres can be fabricated by mimicking the preparation conditions of TiO<sub>2</sub> nanotubes without the electric field. Here, we demonstrate the surface erosion route for the fabrication of anatase TiO<sub>2</sub> hollow spheres.

Herein, we report the synthesis of TiO<sub>2</sub> hollow spheres with a pure phase of anatase via microwave-assisted solvothermal process. A simple surface chemical erosion approach to the preparation of TiO<sub>2</sub> hollow spheres mimicking the preparation conditions of TiO<sub>2</sub> nanotube through the solvothermal process has been developed. We designed a dissolution (inside TiO<sub>2</sub> spherical particles)–recrystallization (on the surface of TiO<sub>2</sub> spherical particles) mechanism

Z. Zhu (✉) · Z. He · J. Li · J. Zhou · N. Wei · D. Liu  
School of Materials Science and Engineering, Shaanxi  
University of Science and Technology, Xi'an 710021,  
People's Republic of China  
e-mail: zhuzf@sust.edu.cn

to explain self-assembled hollow  $\text{TiO}_2$  spheres generated through the surface erosion of  $\text{TiO}_2$  spherical particles by the solvothermal process. The products were characterized by using techniques such as powder X-ray diffraction (XRD), scanning electron microscopy (SEM), and transmission electron microscopy (TEM). And the photocatalytic activity was evaluated by the photocatalytic degradation of methyl orange (MO).

## Experimental

### Preparation

In our experiment, tetrabutyl titanate ( $\text{Ti(OBu)}_4$ ), ethanol, and sodium fluoride, sodium chloride were of analytical grade used without further purification. Distilled water was used throughout the preparation.

The typical experimental procedures are depicted as follows: First, a given amount of  $\text{Ti(OBu)}_4$  was dropwise added into the mixture of ethanol (100 mL) and sodium chloride (0.4 mL, 0.1 M) to obtain a turbid solution under magnetic stirring. Then, the suspension was aged in a static condition for 24 h, the powder deposited at the bottom of the vessel was collected and dried at 80 °C in air; Second, 0.8 g of the obtained  $\text{TiO}_2$  particles and 0.18 g sodium fluoride were dispersed into a mixture of 20 mL ethanol and 10 mL deionized water with the assistance of strong magnetic stirring. After 10 min of stirring, the final mixture was directly transferred into a 100 mL Teflon autoclave. The autoclave was maintained at 180 °C by microwave irradiation for 1 h. After cooled to room temperature, white solid products were obtained by washing with deionized water and ethanol for several times and air drying.

### Characterization

X-ray diffraction (XRD, DX-2200) measurement was performed on a diffractometer with  $\text{Cu K}\alpha$  radiation with  $\lambda = 1.5418 \text{ \AA}$ . Scanning electron microscopy (SEM, JSM-6700F) and transmission electron microscopy (TEM, JEM-3010) were applied to examine the morphology. The BET surface areas of the samples were obtained from  $\text{N}_2$  adsorption/desorption isotherms determined at liquid nitrogen temperature on an automatic analyzer.

### Photocatalytic activity

The photocatalytic activity of the prepared  $\text{TiO}_2$  was evaluated through degradation of 50 mg/L MO in a BL-GHX-V multifunctional photochemical reactor (Shanghai Bilon Experiment Equipment Co. Ltd., Shanghai, China). The volume of the reaction solution was 250 mL (eight text

tubes, every tube 30 mL), into which 100 mg of photocatalyst was added. Irradiation was provided by a medium-pressure Hg lamp (300 W). The solution was dispersed by sonication, and then transferred to text tubes, string was performed all the time during reaction. Sampling was also performed at regular time during reaction. The residue concentration of MO was determined by measuring its absorbance at 460 nm using an UV–Vis spectrophotometer (UV-2550).

## Results and discussion

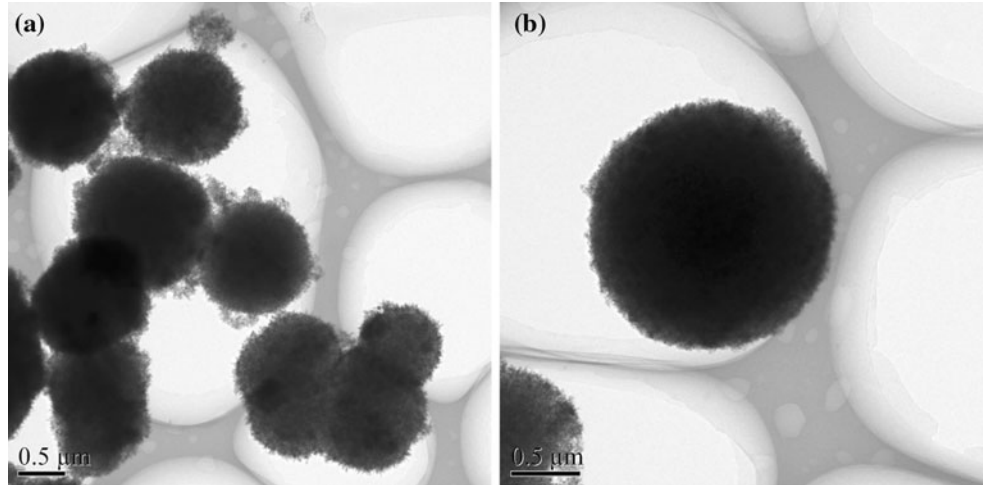
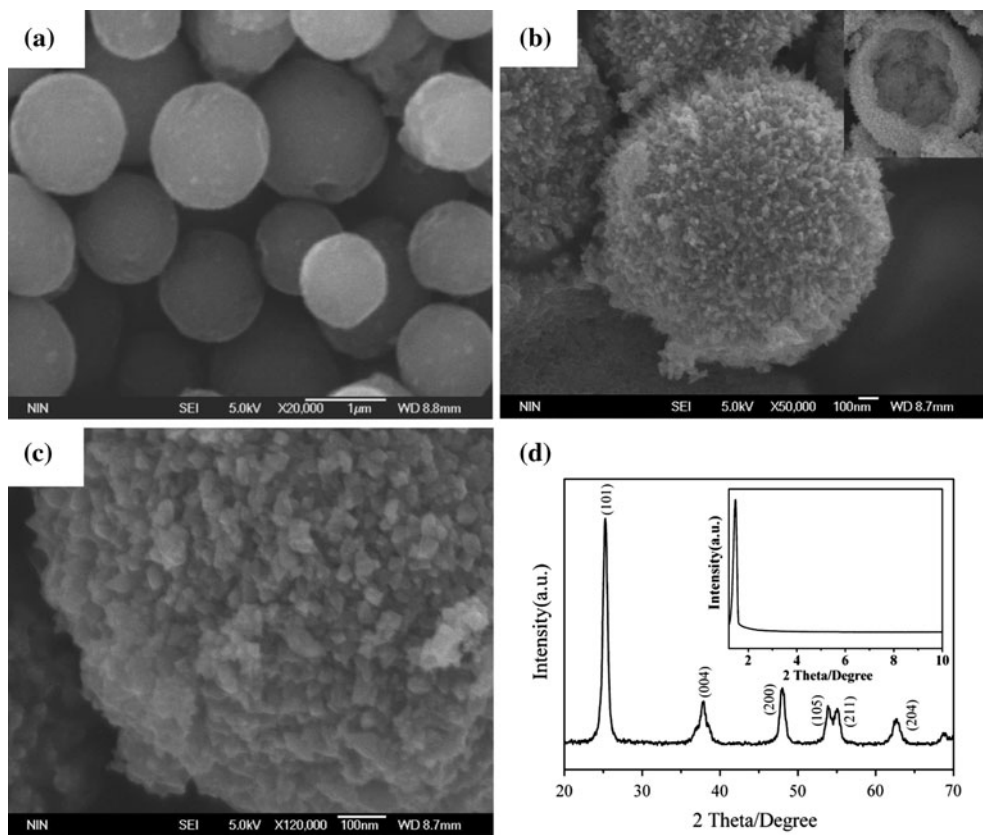
### SEM and XRD analysis

Figure 1 shows SEM images of the as-prepared samples. The  $\text{TiO}_2$  particles before hydrothermal process were shown at Fig. 1a, the sample consisted of solid microspheres with relatively smooth surface. Their diameters were about 800–1200 nm. Interestingly, after the addition of sodium fluoride dopant, the microstructure of the microspheres changed significantly. Hollow structured microspheres and comparatively rough surfaces were produced. Many cracked  $\text{TiO}_2$  spheres showing the hollow cavity can be found in the final samples in Fig. 1b by careful observation, and hollow structured microspheres could be observed in the samples (Fig. 1b, inset). The final samples contained nanocrystals (16–20 nm) could be observed over the surface of the spheres (as shown in Fig. 1c). Figure 1d shows the XRD patterns of the hollow products. The peaks at scattering angles of 25.26°, 36.88°, 47.78°, and 62.74° correspond to the reflections from the (101), (004), (200), and (204) crystal planes of anatase  $\text{TiO}_2$ , respectively. All the peaks can be perfectly indexed as anatase phase of  $\text{TiO}_2$  (JCPDS card No. 21-1272) with lattice constants  $a = 3.7852 \text{ \AA}$ ,  $c = 9.5139 \text{ \AA}$ , all the reflections can be readily indexed as a pure anatase phase of  $\text{TiO}_2$ , and no peak for metallic titanium was observed. The crystal size estimated from the full width at half maximum of the (101) peak using the Scherrer equation indicated that these  $\text{TiO}_2$  nanocrystals were 16.88 nm in diameter, in a good agreement with that measured from SEM images (Fig. 1c). The inset curve implied that the hollow spheres had mesoporous structure.

### TEM analysis

The size and morphology of the as-prepared products were further analyzed by TEM and HRTEM image. The titanium spherical particles before hydrothermal process were shown at Fig. 2, the sample consisted of solid microspheres with relatively smooth surface. Their diameters were about 800–1200 nm, and these spheres did not have hollow structure. As shown in the TEM images in Fig. 3, the

**Fig. 1** **a** SEM image of incompletely reacted  $\text{TiO}_2$  particles at the initial stage, **b**, **c** SEM images of the final product, and **d** XRD patterns showing the existence of final products



**Fig. 2** Low-magnification TEM image (**a**, **b**) of  $\text{TiO}_2$  powder

samples obtained from microwave-assisted solvothermal process consisted of hollow structured spheres, confirming the SEM results. From Fig. 3c, we can clearly see some stripes on the surface of product. Furthermore, the lattice spacing is about  $3.6 \text{ \AA}$  between adjacent lattice planes of the sample (HRTEM image, Fig. 3d), corresponding to the distance between (101) crystal planes of the anatase phase. So it indicated the nanocrystals grow along this direction.

#### BET analysis

Figure 4 shows nitrogen absorption–desorption isotherms (inset) and pore-size distribution plots for the as-synthesized samples. Both samples show a type-IV isotherm, which is representative of mesoporous solids. The specific surface area of the  $\text{TiO}_2$  particles (shown in Fig. 4a) is  $55 \text{ m}^2/\text{g}$  using the Brunauer–Emmett–Teller (BET) method, the pore

**Fig. 3** Low-magnification TEM image (**a**, **b**). Enlarged TEM image and HRTEM image of (**c**, **d**) of the TiO<sub>2</sub> hollow spheres

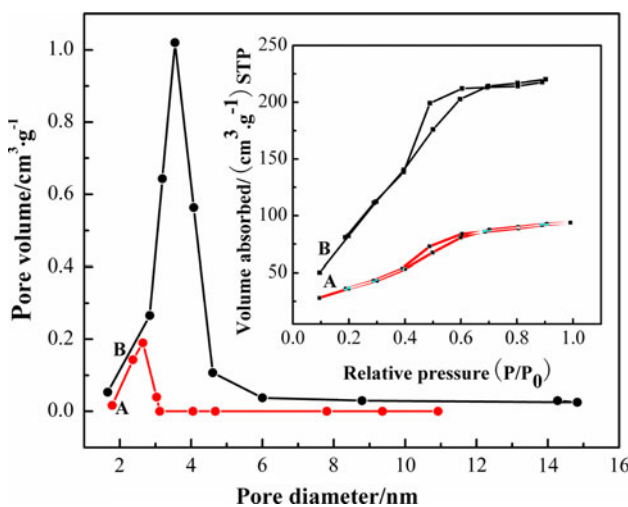
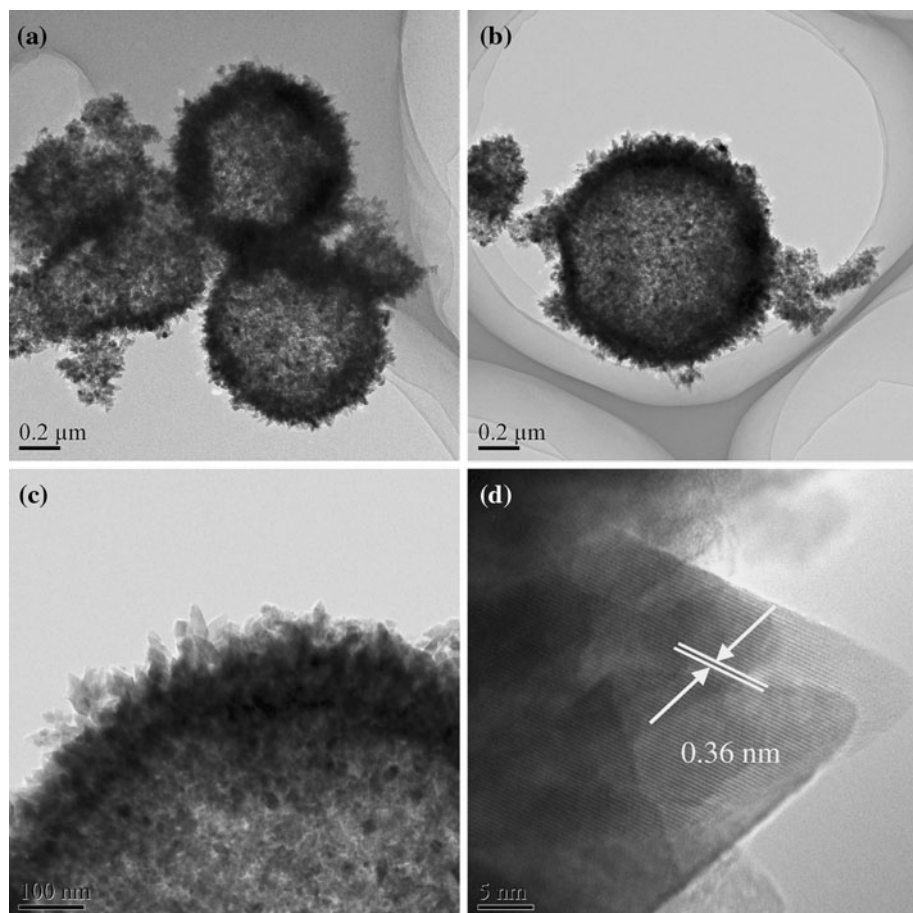


**Fig. 4** **a**, **b** N<sub>2</sub>-sorption isotherms (inset) and corresponding pore-size distribution curves for the TiO<sub>2</sub> particles and TiO<sub>2</sub> hollow microspheres, respectively

diameter is 2.9 nm. The TiO<sub>2</sub> hollow microspheres (Fig. 4b) possesses average pore diameter of 3.6 nm and have relatively high specific surface area (180 m<sup>2</sup>/g). It clearly demonstrates that the microspheres having hollow structure have higher specific surface area.

#### Formation mechanisms of TiO<sub>2</sub> hollow spheres

Herein we consider adsorbed water layers formed on the surface of spherical TiO<sub>2</sub> particles. The formation of a hollow particle is a complicated process involving the diffusion and reactions of several species such as metal oxide particles, and water layer. Here the process is simplified by the following assumptions: The nanometer-sized particles were decomposed inside the spherical TiO<sub>2</sub> particles and transported into water droplet, then aggregated at the interface (the adsorbed water surfaces), and is incorporated into the oxide shell, leading to the growth of shell and closing of pore. The model is schematically illustrated in Fig. 5.

On the basis of the above modeling and observations, we propose possible mechanisms for the formation of hollow structured microspheres via the microwave-assisted solvothermal process combined the sol–gel method.

In such a Ti(OBu)<sub>4</sub>/NaCl/ethanol mixture quasi-nonaqueous system, the alcoholysis of Ti(OBu)<sub>4</sub> initiated tardily at the ambient temperature. The concentration of mineralizing agent (NaCl in here) controlled slow nucleation and growth process of TiO<sub>2</sub> formed small TiO<sub>2</sub> crystallites. Then, these nanometer-sized particles aggregated

**Fig. 5** Schematic illustration of formation model of a hollow particle. Metal oxide particles (A) is partially decomposed inside the spherical  $\text{TiO}_2$  particles and transported into water shell, then aggregated at the interface, and is incorporated into the shell of metal oxide (S). The production of S near the interface leads to the growth of shell and closing of pore

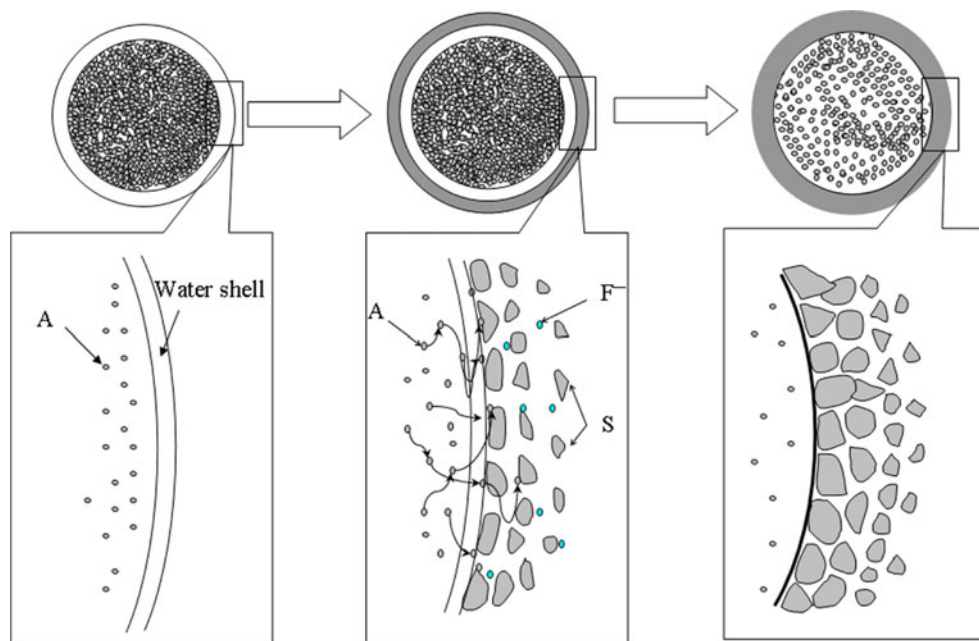
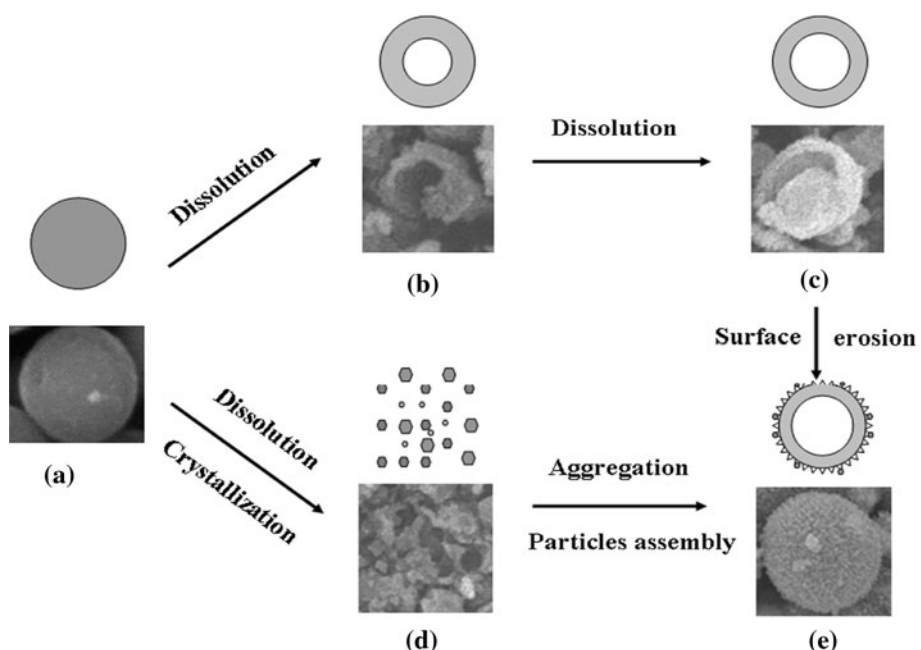


**Fig. 6** Schematic showing the two dissolution–crystallization process for the formation of  $\text{TiO}_2$  hollow sphere: **a**  $\text{TiO}_2$  spherical particles, **b** dense  $\text{TiO}_2$  shell, **c** thinner  $\text{TiO}_2$  shell, **d** formation and assembly of  $\text{TiO}_2$  nanoparticles into hollow hemispheres, and **e**  $\text{TiO}_2$  hollow spheres



isotropically to form the spherical product due to a well-known aggregation mechanism [17, 18]. After the air drying, the amorphous  $\text{TiO}_2$  spherical particles were prepared. The plausible reactions of formation of  $\text{TiO}_2$  spherical particles in this process are proposed as follows:



The schematic illustration for the formation of  $\text{TiO}_2$  hollow spheres under solvothermal process is depicted in Fig. 6. The microwave-assisted solvothermal process began with homogeneous aqueous solution containing soluble precursors. Consequently, the precursor ions ( $\text{Ti}^{4+}$ ,  $(\text{OBu})_4^-$ , and  $\text{H}_3\text{O}^+$  ions) would gradually assemble in the interior layer of the spherical  $\text{TiO}_2$  particles via the diffusion process and the solvent evaporation would happen simultaneously. Then the dissolution inside  $\text{TiO}_2$  spherical particles and the

NaF molecules dissociation would happen when heated in the autoclave.

During the microwave-assisted solvothermal process, the plausible reactions of formation of  $\text{TiO}_2$  hollow spheres on the  $\text{TiO}_2$  spherical particles in the presence of ethanol and sodium fluoride during the solvothermal process are proposed as follows [19]:



On the basis of the modeling in Fig. 5, we propose possible mechanisms for the formation of hollow structured microspheres. Tips and defects of the  $\text{TiO}_2$  spherical particles present a high local charge density and a strong electrostatic field and generate the adsorbed water layer on the surface of  $\text{TiO}_2$  particles [20, 21], which promotes water and NaF molecules dissociation. It is evident that the formation of adsorbed water layer on the  $\text{TiO}_2$  spherical particles surface experienced the dissolution of  $\text{TiO}_2$  spherical particles. It is well-known that metallic titanium has high susceptibility to pitting corrosion by fluoride ion attacking [22], further study shows the formation of  $\text{TiO}_2$  nanotubes is due to the directional etching of titanium oxide induced by fluoride ion pitting corrosion under the external electric field [23]. In the present solvothermal synthesis, hydrogen fluoride generated from the dissociation reaction of titanium fluoride can react with the  $\text{TiO}_2$  on the surface of  $\text{TiO}_2$  spherical particles, then  $\text{TiF}_4$  was formed by the dissolution of the dense  $\text{TiO}_2$ , hydrolysis of  $\text{TiF}_4$  further form  $\text{TiO}_2$  nanometer-sized particles. Simultaneously, the  $\text{TiO}_2$  spherical particles were partly decomposed into nanoparticles, especially inside the shell, so the shell was formed. Then the nanometer-sized particles accelerated to result in the formation of  $\text{TiO}_2$  nuclei. The  $\text{TiO}_2$  nuclei were formed and grew on the malformed shell of spheres. As shown in Fig. 1c, numerous small titanium dioxide nanometer-sized particles nucleated on the surface of  $\text{TiO}_2$  spherical particles due to the hydrolysis reactions of the high concentration  $\text{TiF}_4$  [24]. By aging in the autoclave, the hollow  $\text{TiO}_2$  spheres were formed finally as shown in Figs. 5 and 6.

#### Photocatalytic activity

It has been reported that the anatase phase has some photocatalytic activity for degrading the organic dye MO, so the photocatalytic activity of our anatase  $\text{TiO}_2$  hollow spheres was also evaluated from MO degradation. The

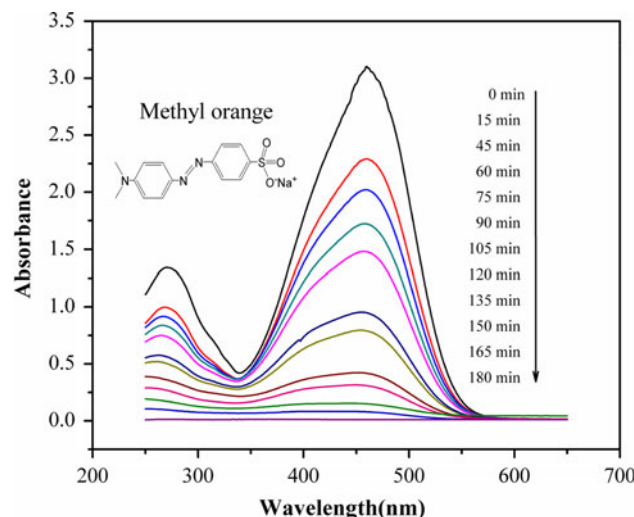


**Fig. 7** Successive UV-Vis spectra of MO photocatalytic degradation in the presence of the sample under UV irradiation. The concentration of the reactants was as follow: [MO] = 50 mg/L, [ $\text{TiO}_2$  hollow spheres] = 0.1 g/L

kinetics of this reaction can be monitored by UV-Vis spectroscopy as seen from UV-Vis spectra measured at different times shown in Fig. 7. It demonstrates MO shows a strong absorption band at 460 nm and the addition of  $\text{TiO}_2$  hollow spheres leads to a decrease of the absorption band with time. The color of the dispersion disappeared after the reaction, indicating that the chromophoric structure of the dye was destroyed. Additional experiments demonstrated that degradation of MO is negligible in the absence of photocatalyst. The order rate kinetics with respect to the MO concentration could be used to evaluate the photocatalytic rate as done previously. As it clearly demonstrated the  $\text{TiO}_2$  hollow spherical nanoparticles show higher photocatalytic activity. The photocatalytic can be attribute to the doped F atoms, because the doped F atoms convert  $\text{Ti}^{4+}$  to  $\text{Ti}^{3+}$  by charge compensation and that the presence of a certain amount of  $\text{Ti}^{3+}$  reduces the electron-hole recombination rate and thus enhances the photocatalytic activity [25]. The creation of oxygen vacancies and the specific surface area can also induce the photocatalytic activity [26].

#### Conclusion

In summary, we have described the two-step template-free facile surface erosion route to the preparation of  $\text{TiO}_2$  hollow spheres. The results indicate that the anatase-type assembly  $\text{TiO}_2$  spheres with special hollow structure and higher photocatalytic activity are successfully synthesized by microwave-assisted solvothermal process. In this process, the nanometer-sized particles were formed inside the

TiO<sub>2</sub> spherical particles, and assembled at the aggregation center and gradually formed TiO<sub>2</sub> hollow spheres. The detailed dissolution-crystallization mechanism for the formation of TiO<sub>2</sub> hollow spheres was also proposed.

**Acknowledgements** This research was financially supported by the Doctoral Research Start-up Fund of Shaanxi University of Science and Technology (BJ08-01), Special Fund from Shaanxi Provincial Department of Education (09JK352), and the Graduate Innovation Found of Shaanxi University of Science and Technology.

## References

1. Chae SY, Park MK, Lee SK, Kim TY, Kim SK, Lee WI (2003) Chem Mater 15:3326
2. Liu Q, Huang H, Lai L et al (2009) J Mater Sci 44(5):1187. doi:[10.1007/s10853-009-3268-3](https://doi.org/10.1007/s10853-009-3268-3)
3. Toma SH, Toma HE (2006) Electrochim Commun 8:1628
4. Qiao H, Zheng Z, Zhang LZ et al (2008) J Mater Sci 43(8):2778. doi:[10.1007/s10853-008-2510-8](https://doi.org/10.1007/s10853-008-2510-8)
5. Zhao W, Song XY, Chen GZ et al (2009) J Mater Sci 44(12):3082. doi:[10.1007/s10853-009-3410-2](https://doi.org/10.1007/s10853-009-3410-2)
6. Song YT, Wei JJ, Yang YZ et al (2010) J Mater Sci 45(15):4158. doi:[10.1007/s10853-010-4505-5](https://doi.org/10.1007/s10853-010-4505-5)
7. Lu BW, Endo A, Inagi Y et al (2009) J Mater Sci 44(24):6463. doi:[10.1007/s10853-009-3627-0](https://doi.org/10.1007/s10853-009-3627-0)
8. Zhang YY, Liu JL, Zhu YX et al (2009) J Mater Sci 44(13):3364. doi:[10.1007/s10853-009-3439-2](https://doi.org/10.1007/s10853-009-3439-2)
9. Koo HJ, Kim YJ, Lee YH, Lee WI, Kim K, Park NG (2008) Adv Mater 20:195
10. Huang NP, Michel R, Voros J, Textor M, Hofer R, Rossi A, Elbert DL, Hubbell JA, Spencer ND (2001) Langmuir 17:489
11. Kim YJ, Chai SY, Lee WI (2007) Langmuir 23:9567
12. Nakashima T, Kimizuka N (2003) J Am Chem Soc 125:6386
13. Liu ZY, Sun DD, Guo PJ, Leckie O (2007) Chem Eur J 13:1851
14. Yang HG, Zeng HC (2004) J Phys Chem B 108:3492
15. Li XX, Xiong YJ, Li ZQ, Xie Y (2006) Inorg Chem 45:3493
16. Zhou JK, Lv L, Yu JQ, Li HL, Guo PZ, Sun H, Zhao XS (2008) J Phys Chem C 112:5316
17. Boissiere C, van der Lee A, El Mansouri A, Larbot A, Prouzet E (1999) Chem Commun 2047
18. Ocana M, Rodriguez-Clemente R, Serna CJ (1995) Adv Mater 7:212
19. Liu B, Zeng HC (2004) J Am Chem Soc 126:8124
20. Mao YB, Kanungo M, Benny TH, Wong SS (2006) J Phys Chem B 110:702
21. Zhou XF, Chen Y, Mei H, Hu ZL, Fan YQ (2008) Appl Surf Sci 255:2803
22. Casillas N, Charlebois S, Smyrl WH, White HS (1994) J Electrochem Soc 141:636
23. Mor GK, Varghese OK, Paulose M, Shankar K, Grimes CA (2006) Sol Energy Mater Sol Cells 90:2011
24. Li J, Zeng HC (2007) J Am Chem Soc 129:15839
25. Yu JC, Yu JG, Ho WK, Jiang ZT, Zhang LZ (2002) Chem Mater 14:3808
26. Li D, Haneda H, Hishita S, Ohashi N, Labhsetwar NK (2005) J Fluorine Chem 126:69